Journal of Wind Engineering and Industrial Aerodynamics, 49 (1993) 311–318
Elsevier

Base Pressure Coefficients for Flows around Rectangular Plates

K. Hourigan[a], R. Mills[b], M.C. Thompson[a], J. Sheridan[b], P. Dilin[c] and M.C. Welsh[a]

[a] Commonwealth Scientific and Industrial Research Organisation (CSIRO), Division of Building, Construction and Engineering, P.O. Box 56, Highett, Victoria 3190, AUSTRALIA

[b] Department of Mechanical Engineering, Monash University, Clayton, Victoria 3168, AUSTRALIA

[c] Department of Mechanical Engineering, Huainan Mining Institute, Anhui Province, PEOPLE'S REPUBLIC OF CHINA.

Abstract

The flow around long rectangular plates can be modified by acoustic forcing. The leading-edge vortex shedding is locked to the sound frequency over a broad range of flow velocities. Close to a critical acoustic Strouhal number, significant drops in the mean base pressure coefficient may occur, depending on the plate chord. It is hypothesised that the plate chord changes the position in the acoustic phase at which the leading-edge vortices arrive at the trailing edge. Interference with the trailing-edge vortex shedding may then be responsible for the significant variation in mean base pressure coefficient. This situation is not observed for flows around plates with no leading-edge shedding.

Nomenclature

c	plate chord (mm)
$C_p = p_s/(1/2\rho U^2)$	time mean local surface pressure coefficient
$C_{p,B}$	time-mean base pressure coefficient at midspan
$Eu = p/(\rho U^2)$	Euler number
f	acoustic frequency (Hz)
p	acoustic pressure (Pa)
p_s	surface pressure (Pa)
$St = ft/U$	acoustic Strouhal number
t	plate thickness (mm)
u'	acoustic particle velocity amplitude (m s^{-1})
U	freestream flow velocity (m s^{-1})
ρ	fluid density (kg m^{-3})

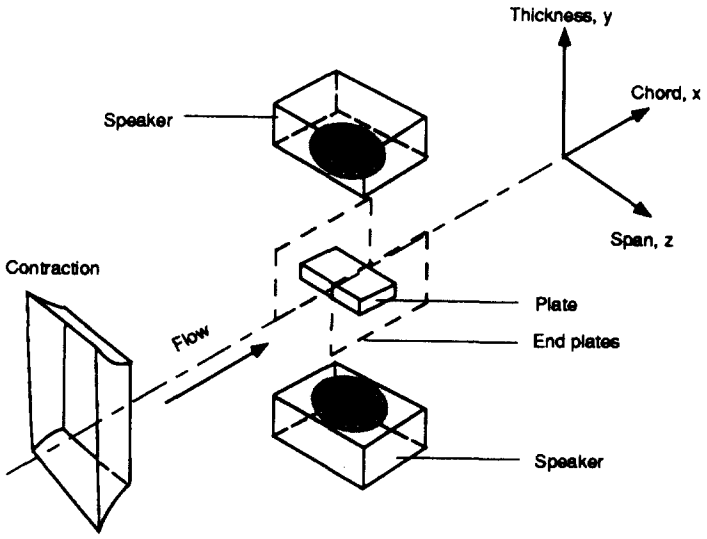

Figure 1: Schematic of the working section of the open-jet wind tunnel with speakers and plate installed.

Plate Dimensions

The basic rectangular test plate was 13 mm thick (t), 135 mm span and 130 mm chord (L) and was mounted with endplates in an open jet wind tunnel (Fig. 1). The plates were mounted on the centreline of the jet, and set at zero incidence angle to the flow. The chord of the plate was adjusted by affixing extra plates of identical thickness to the leading edge.

Instrumentation

Loudspeakers were placed above and below the plates outside the jet to generate a transverse velocity perturbation at an adjustable amplitude and frequency. The loudspeakers were connected in anti-phase to a stereo audio amplifier and the sound pressure level on the top and bottom surfaces of the plate was adjusted with the aid of a microphone. The applied sound frequency was adjusted using a signal generator. The local pressure coefficients along the plate surface were measured for different values of these parameters and for different plate lengths.

For the wind tunnel experiments, the plates had pressure tappings along the leading and trailing edges in addition to tappings along one of the long sides. A row of 27 pressure tappings was located on the top surface along the midspan of the basic plate, with tappings at approximately 1.5 mm from the leading and trailing edges of the plate at midspan and 13 tappings were positioned spanwise along the centreline of the trailing edge of the plate. These surface tappings were connected to a Setra low differential pressure transducer via

a Scanivalve. The signals were sampled and processed by a PDP11/44 computer using high-speed logging software. The pressure transducer had a differential pressure range -105 to 140 Pa and an accuracy to within ±0.5 Pa.

A probe microphone was located 65 mm downstream of the trailing edge of the plate and 13 mm above the level of the plate top surface to measure the frequency of the vortex street. The data from the probe microphone were analysed using a PDP 11/44 computer with an LPA 11 analog-to-digital converter with ILS (Interactive Laboratories Systems) software. The signals were sampled over a period of 32 seconds and digitised at 800 Hz after band passing between 0 and 1000 Hz. The frequencies of the spectral peaks, corresponding to the sound and the vortex shedding, were obtained after averaging 50 spectra, which were each determined using a ninth order Fast Fourier Transform.

The resonant characteristics of the probe microphones were checked before the experiments. A probe microphone and a 12.7 mm diameter microphone were located close to each other near a white noise sound source to get the coherence and the transfer functions between the two microphones. The transfer function was fairly smooth and there was no peak in the frequency range of 60 to 250 Hz.

The background noise level inside the laboratory was at least 40 dB less than the major spectral peaks.

3. RESULTS and DISCUSSION

Physical experiments have been undertaken to date for rectangular plates with chord-to-thickness ratios of 10, 13 and 15.

The Euler number Eu is proportional to the square of the ratio of the acoustic particle velocity amplitude to the freestream velocity. For a constant Euler number, the relative acoustic forcing is constant. As a reference value, for a flow speed of 8.77 m s^{-1} and sound applied at 115 dB, the Euler number is 0.122 and the acoustic particle velocity amplitude, u', 0.5 mm upstream of the leading-edge time-mean stagnation point is 0.043 U. This value of the amplitude was determined using laser doppler velocimetry, as described by Welch *et al.* [10].

For a given plate chord-to-thickness ratio and constant relative acoustic forcing (reflected by a constant Euler number), the surface pressure coefficient along the plate is similar for different flow velocities (see Fig. 2). This similarity over a range of Reynolds number is typical of bluff-body flows and enables reasonable generalisation of the results.

When sound is applied at the critical acoustic Strouhal number 0.17 and Euler number 0.076 (i.e. $u'/U = 0.034$) in the case of a plate with chord-to-thickness 10, a significant reduction in the local pressure coefficients along the trailing edge of the basic plate is observed (Fig. 3).

The variation in the mean base pressure coefficient as the acoustic Strouhal number is varied for different plate lengths is shown in Fig. 4.

For plate chord-to-thickness ratios of 10 and 15, there is a single minimum in the mean base pressure coefficient, occuring at an acoustic Strouhal number of approximately 0.17. However, for an intermediate plate chord-to-thickness ratio of 13, a recovery in the base pressure coefficient is observed at this critical acoustic Strouhal number. Corresponding experiments carried out with plates having aerofoil-shaped leading edges did not show this sensitivity of the mean base pressure coefficient to the chord-to-thickness ratio. This

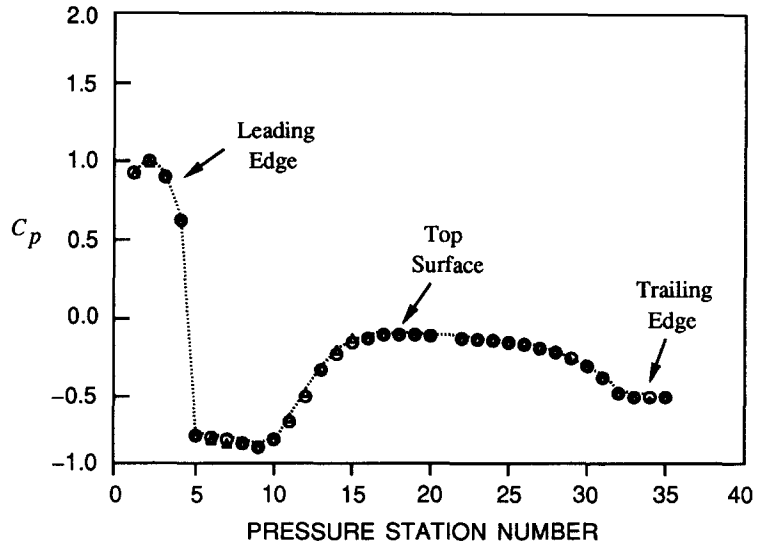

Figure 2: Surface pressure coefficient, C_p, at different measuring stations along the plate surface for chord-to-thickness ratio 10, Euler number 0.076, acoustic Strouhal number 0.17, at 2 different flow velocities : ◯, $U = 11.1$ m s^{-1}; △, $U = 8.7$ m s^{-1}.

evidence supports the hypothesis that some interference is occuring between the leading-edge vortices and the trailing-edge vortex shedding. The occurrence of minima, at the same critical Strouhal number, in the mean base pressure coefficient profile at chord-to-thickness ratios 10 and 15 suggests a periodicity of the order 5 plate thicknesses. Assuming the vortex velocity along the plate surface is 0.75 U, then the spacing between vortices for an acoustic Strouhal number of 0.17 is approximately 4.5 plate thicknesses. This is again consistent with the hypothesis of vortex interference.

Fig. 5 shows the averaged spectra from the probe microphone signal for the different length plates. These spectra are plotted to an uncalibrated linear scale. The flow velocity, the applied sound frequency and the sound pressure level were all kept constant at 10.2 m s^{-1}, 135 Hz, and 115 dB, respectively, when the spectra were taken for the different length plates. The acoustic Strouhal number under these conditions is the critical value of 0.17. Although the fluctuations in the wakes have the same frequency, the spectral peaks at the vortex shedding frequency are significantly different. The peaks in the spectra for the shortest and longest plates ($c/t = 10$ and $c/t = 15$) are higher than the peak in the spectrum for the intermediate length plate ($c/t = 13$).

The base pressure results and the probe microphone results are consistent in suggesting less vigorous vortex shedding at the trailing edge for the flow around the intermediate length plate at the critical Strouhal number of 0.17.

From the water-tunnel experiments, the wake consists of large-scale structures originating from the leading-edge shedding in addition to shedding from the trailing edge which

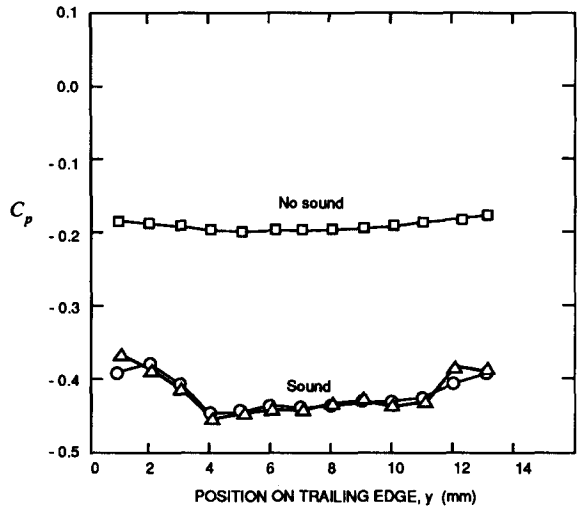

Figure 3: Surface pressure coefficient, C_p, at different measuring stations along the plate trailing edge for chord-to-thickness ratio 10, acoustic Strouhal number 0.17, for no applied sound: □, $U = 10.3$ m s^{-1}; and for sound, Euler number 0.076, at 2 different flow velocities: ○, $U = 11.1$ m s^{-1}; △, $U = 8.7$ m s^{-1}.

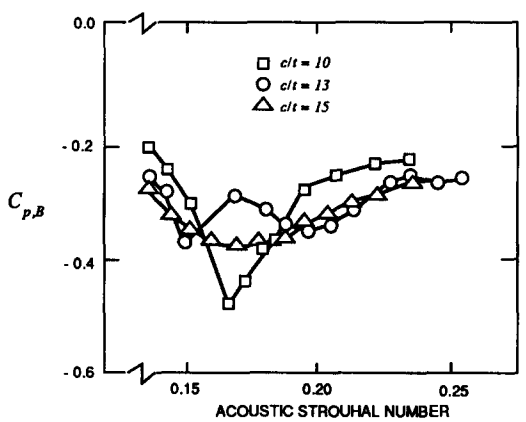

Figure 4: Time-mean base pressure coefficient, $C_{p,B}$, Euler number 0.076, flow velocity $U = 10.2$ m s^{-1}, versus acoustic Strouhal number for 3 different plate chord-to-thickness ratios: □, $c/t = 10$; ○, $c/t = 13$; △, $c/t = 15$.

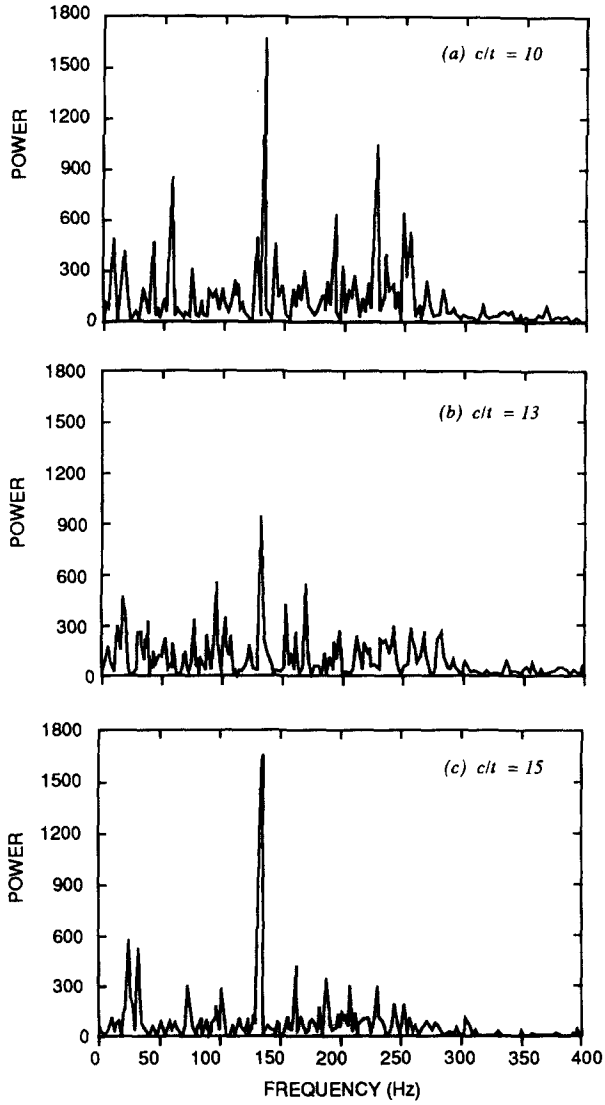

Figure 5: Averaged spectra (uncalibrated units) from the probe microphone placed downstream of the trailing edge for different plate lengths when sound was applied at 115 dB and 140 Hz for a flow velocity 10.2 m s^{-1}.

(a)

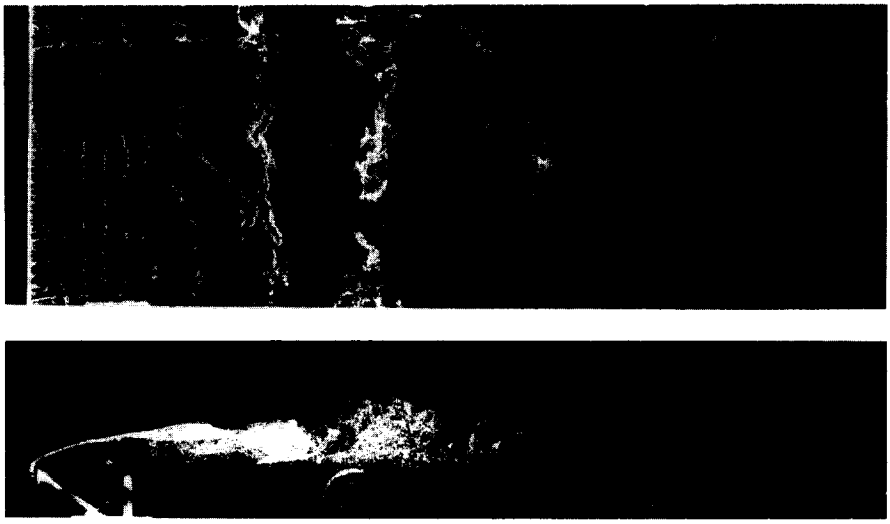

(b)

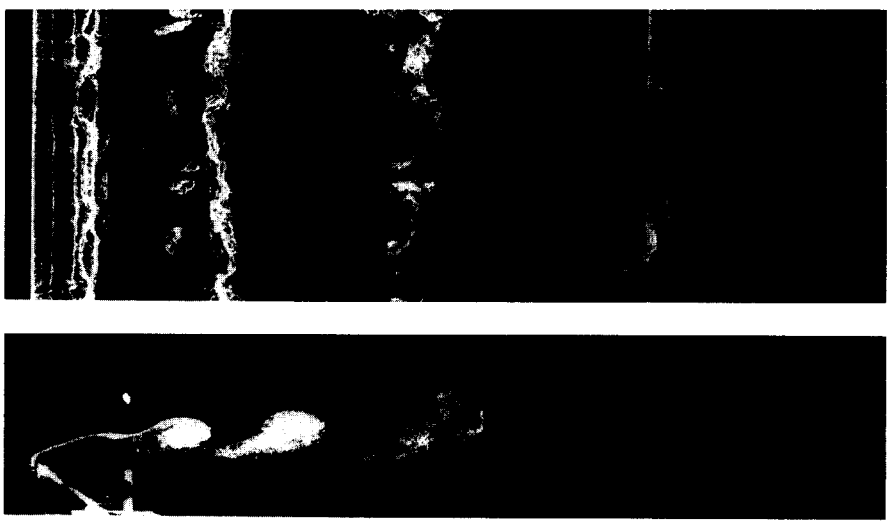

Figure 6: Visualisation of plan view and side view (not at same instant of time) using hydrogen bubbles for flow, Reynolds number of 1300 based on plate thickness, around a rectangular plate, chord-to-thickness ratio 10, with: (a) no perturbation; and (b) transverse velocity perturbation at forcing Strouhal number 0.2.

is more difficult to visualise (Fig. 6). Evidently, hairpin vortices develop across the span of the large-scale structures. Video recordings of the flow over the plate in a water tunnel show that when the flow is forced in a manner analogous to the acoustic forcing in the wind tunnel, vigorous vortex shedding at the trailing edge is observed near the critical forcing Strouhal number. This provides evidence for the hypothesis that the trailing-edge vortex shedding can be locked to the forcing, leading to reduced wake formation length and increased drag.

4. CONCLUSIONS

Evidence has been obtained experimentally that the mean base pressure coefficient can be modified substantially when transverse forcing is applied to the flow around rectangular plates. Transverse forcing can lock the vortex shedding from both the leading and trailing edges. For the plate chord-to-thickness ratios considered, the vortex structures shed from the leading edge remain individual entities while convecting to the trailing edge. A substantial decrease in the the base pressure coefficient occurs when the forcing frequency approaches the critical Strouhal shedding number (approximately 0.17), for flows around plates with chord-to-thickness ratios 10 and 15. However, a recovery in the base pressure coefficient is observed for the plate with chord-to-thickness ratio 13, for which the spectral peak in fluctuating pressure, measured in the wake, at the forcing frequency is also reduced. It is suggested that when both the leading-edge and trailing-edge vortex shedding are locked to the forcing frequency, which occurs near the critical Strouhal number of 0.17, substantial interference to the trailing-edge shedding can occur.

Acknowledgement
This work is continuing with the support of a grant from the Australian Research Council.

5. REFERENCES

1 P.I. Cooper, J.C. Sheridan and G.J. Flood, The Effect of Sound on Forced Convection Over a Flat Plate, International Journal of Heat and Fluid Flow, 7 (1986) 61.
2 K. Hourigan, L.W. Welch, M.C. Thompson, P.I. Cooper and M.C. Welsh, Exp. Thermal and Fluid Science, 4 (1990) 182.
3 T. Ota and N. Kon, Int. J. Heat and Mass Transfer, 22 (1979) 197.
4 A. Roshko, J. Aero. Sc., 22 (1955) 124.
5 P.W. Bearman, J. Fluid Mech., 21 (1965) 241.
6 P.W. Bearman, The Aeronautical Quart., 18 (1967) 207.
7 M.C. Welsh and D.C. Gibson, J. Sound and Vibration, 67 (1979) 501.
8 A.N. Stokes and M.C. Welsh, Journal of Sound and Vibration, 104 (1986) 55.
9 M.C. Welsh, K.Hourigan, L.W. Welch, R.J. Downie, M.C.Thompson and A.N. Stokes, Exp. Thermal and Fluid Science, 3 (1990) 138.
10 L.W. Welch, C.J. Carra and K. Hourigan, 9th Aust. Fluid Mech. Conf., University of Auckland, 8-12 Dec. (1986) 39.